International Journal of Infrared and Millimeter Waves, Vol. 11, No. 7, 1990

ANALYSIS OF A CONICAL HORN FED BY A SLIGHTLY OVERSIZED WAVEGUIDE

S. A. Torchinsky

Department of Astronomy
University of Edinburgh
Blackford Hill, Edinburgh, EH9 3HJ, Scotland

Received April 1, 1990

Abstract

This paper discusses the case of a submillimetre conical feedhorn system which is overmoded due to an oversized waveguide, but is not in the geometric optics regime. The motivation for this system is to use the same feed as a multi-frequency receiver. Increased background loading is the greatest disadvantage in overmoded optics; and aperture efficiency also suffers due to non-optimum horn dimensions. The analysis is done using the Laguerre-Gauss beam expansion method.

KEYWORDS: OVERSIZED WAVEGUIDE, OVERMODED, CONICAL HORN, QUASI-OPTICS

1 Introduction

Nearly thirty years ago Taub *et al.* [1] established the viability of using oversized waveguides. In that work an oversized circular waveguide was shown to propagate a TE_{11} beam mode without significant attenuation over a long distance. Note that although the guide was oversized, it was not overmoded. More recently, Crenn [2] , and Belland & Crenn [3] have considered the problem of an oversized and overmoded circular waveguide, in which a Gaussian beam is propagated through the guide. Theirs is an analysis in the geometrical limit, and also a "slightly diffracted" beam. The present paper investigates the problem of a very diffracted beam (the horn is fed by a *slightly* oversized waveguide).

Feedhorn for incoherent detectors are generally designed to focus the maximum available power onto a bolometer which then absorbs it, regardless of phase. Often, the horn used to focus energy on the bolometer is an "Ideal Light Collector"

0195-9271/90/0700-0791$06.00/0

or Winston Cone [4,5]. However, optimization of aperture efficiency and reduction of unwanted background power entering the system requires the use of single moded optics. Hence, at submillimeter wavelengths, the antenna is a single moded feedhorn. The conical horn has the problem of differing E and H plane profiles and somewhat non-Gaussian antenna beam profile. This is normally overcome by corrugating the feed resulting in a highly Gaussian field with suppressed sidelobes [6,7]. Unfortunately, manufacturing corrugated feeds for use in the submillimeter waveband is extremely difficult due to their small dimensions, and this is especially prohibitive when many horn antennæ are required. This paper addresses the problem of aperture and beam efficiency in a conical feedhorn system for use in a total power detector.

Presently at the Royal Observatory, Edinburgh, a new receiver is being built for the James Clerk Maxwell Telescope (JCMT) on Mauna Kea, Hawaii. The Submillimetre Common User Bolometer Array (SCUBA) was originally intended to be a two-channel imaging array for simultaneous observations at $350\,GHz$ ($855\mu m$) and $685\,GHz$ ($438\mu m$). However, the astronomical community soon expressed disappointment that the receiver would not also take advantage of two other observing windows that Mauna Kea can offer: $428\,GHz$ ($700\mu m$) and $857\,GHz$ ($350\mu m$). Two options were proposed to give SCUBA this added flexibility. The possibility of including two additional arrays (four altogether) was quickly rejected as this would require complicated optics in order to split the beam into four paths. Instead, SCUBA now has a filter carousel which will allow the astronomer to choose the waveband at which she will observe[8]. Each array of bolometers is designed to have optimum efficiency at the original frequencies of $350\,GHz$ ($855\mu m$) and $685\,GHz$ ($438\mu m$) respectively. The added channels will operate at a non-optimum design, on the first two arrays, and thus the feeds at $428\,GHz$ ($700\mu m$) and $857\,GHz$ ($350\mu m$) will be overmoded.

Section 2 addresses the problem of synthesizing the field profile of the horn using cylindrical waveguide modes for the "source" functions and Gaussian beam analysis to find the far-field profile. The aperture efficiency and beam, or spillover efficiency, are discussed in Section 3, also using Gaussian beam analysis, and Table 2 lists the efficiencies of the waveguide modes for the particular case of $855\mu m$ conical feedhorn used at both its designed wavelength of $855\mu m$ and also at $700\mu m$. Section 4 discusses signal measurement, using a typical astronomical source as an example. The overall conclusion seems to be that the less than optimum efficiencies in the overmoded optics are still sufficient to make overmoded optics a viable method of increasing the flexibility of a receiver, if one is willing to lose out in terms of background loading. For the particular case of SCUBA, the filter carousel is a valid solution to the problem of increasing the instrument from a two to a four-waveband receiver.

2 Profile Synthesis

The far-field horn profile is determined using the method described by Ludwig [9] in conjunction with Gaussian beam analysis [10]. The usual TE_{nm} amd TM_{nm} cylindrical waveguide modes are considered the "source functions" which are then components of the far field profile. Laguerre-Gaussian beam mode analysis is very useful for determining beam truncation and beam profile throughout an optical train. For these reasons, L-G beams are employed in this analysis instead of simply Fourier transforming the horn field to get the far-field profile through a telescope.

The electric fields of the TE_{nm} and TM_{nm} modes are the following:

$$\vec{\mathbf{E}}_{nm}^{\,\mathrm{TE}} = \left[J_{n-1}\left(\gamma_{nm}\frac{r}{a}\right) e^{i(n-1)\theta} + J_{n+1}\left(\gamma_{nm}\frac{r}{a}\right) e^{i(n+1)\theta}\right]\hat{x}$$

$$+ \left[J_{n-1}\left(\gamma_{nm}\frac{r}{a}\right) e^{i(n-1)\theta} - J_{n+1}\left(\gamma_{nm}\frac{r}{a}\right) e^{i(n+1)\theta}\right]\hat{y} \tag{1a}$$

$$\vec{\mathbf{E}}_{nm}^{\,\mathrm{TM}} = \left[J_{n-1}\left(\gamma_{nm}\frac{r}{a}\right) e^{i(n-1)\theta} - J_{n+1}\left(\gamma_{nm}\frac{r}{a}\right) e^{i(n+1)\theta}\right]\hat{x}$$

$$+ \left[J_{n-1}\left(\gamma_{nm}\frac{r}{a}\right) e^{i(n-1)\theta} + J_{n+1}\left(\gamma_{nm}\frac{r}{a}\right) e^{i(n-1)\theta}\right]\hat{y} \tag{1b}$$

$$+ J_n\left(\gamma_{nm}\frac{r}{a}\right) e^{in\theta}\hat{z}$$

The power in each cylindrical wave mode is the integrated Poynting vector over the cross section of the guide:

$$P_{nm} = \frac{1}{\pi a^2}\int_0^a \int_0^{2\pi} r\,d\theta\,dr\ \vec{\mathbf{e}}_{nm} \times \vec{\mathbf{h}}_{nm}^{\,*}$$

$$= \int_0^1 \rho\,d\rho\left[J_{n-1}^2(\gamma_{nm}\rho) + J_{n+1}^2(\gamma_{nm}\rho)\right], \tag{1c}$$

and this will be used to normalize each waveguide mode to unit power. For the TE_{nm} modes, the γ_{nm} are the m^{th} zero of the first derivative *w.r.t.* the argument of Bessel function order n, and for the TM_{nm} modes they are the m^{th} zero of Bessel function order n.

The exact field distribution within the guide is a linear combination of the TE_{nm} and TM_{nm} fields. For a conical horn of small flare angle, the field at the horn mouth can be taken as the waveguide field propagated as a spherical wave from

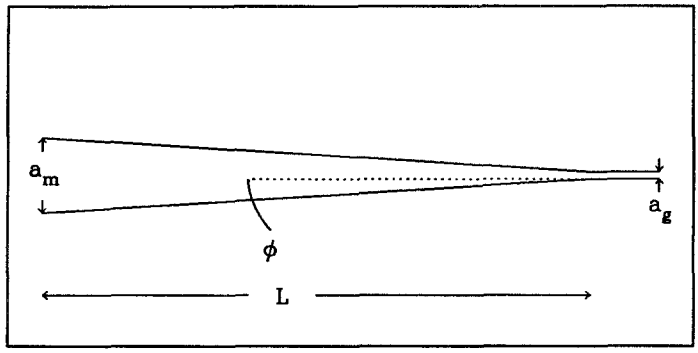

Figure 1: The Conical Feedhorn System

the horn exit to the horn mouth. This gives the usual conical horn approximation of

$$\vec{\mathbf{E}}_{\text{horn}} = \vec{\mathbf{E}}_{\text{guide}} \exp(ikr^2/2L) \tag{2}$$

$$= \sum_{n}^{\infty}\sum_{m}^{\infty} A_{nm}\, \vec{\mathbf{E}}^{\text{TE}}_{nm} \exp(ikr^2/2L) + \sum_{n}^{\infty}\sum_{m}^{\infty} B_{nm}\, \vec{\mathbf{E}}^{\text{TM}}_{nm} \exp(ikr^2/2L)$$

where k is the free space wave number $2\pi/\lambda$, and L is the axial length of the horn (see Figure 1).

Equation 2 is referred to as the "source" functions for generating the antenna beam profile [9]. The A_{nm} and B_{nm} are the Fourier coefficients of the field distribution in terms of the cylindrical waveguide modes, *viz.*

$$A_{nm} = \left\langle \vec{\mathcal{F}}_{\mathbf{S}} \left| \vec{\mathbf{E}}^{\text{TE}}_{nm} \exp(-i\frac{kr^2}{2L}) \right] _{\text{farfield}} \right\rangle \tag{3a}$$

$$B_{nm} = \left\langle \vec{\mathcal{F}}_{\mathbf{S}} \left| \vec{\mathbf{E}}^{\text{TM}}_{nm} \exp(i\frac{kr^2}{2L}) \right] _{\text{farfield}} \right\rangle \tag{3b}$$

$\mathcal{F}_s$ is the field of the emitting source in the far-field of the telescope. The far-field profile of Eq. 2 are determined by L-G beam expansion

$$\Psi_{nm} = N_{nm} \left(\frac{2r^2}{W^2}\right)^{n/2} L_{nm}\left(\frac{2r^2}{W^2}\right) \exp\left(-\frac{r^2}{W^2} + i\frac{kr^2}{2R} + i\Phi + in\theta + ikz\right) \quad (4a)$$

where the Laguerre polynomials are given by the generating function

$$L_{nm}(\zeta) = \frac{e^{\zeta}}{(n+m)!}\frac{d^m}{d\zeta^{n+m}}\left(e^{-\zeta}\zeta^m\right), \quad (4b)$$

and

$$W = W_o\sqrt{1 + (\lambda z/\pi W_o^2)^2}, \quad (4c)$$

$$R = z\left[1 + (\pi W_o^2/\lambda z)^2\right]. \quad (4d)$$

W_o is the beam waist radius which occurs at the focus of the L-G beam ($z = 0$), and Φ is the phase slippage, in addition to that of a spherical wave, relative to the fundamental L-G mode,

$$\Phi = (2m + n)\mathrm{Tan}^{-1}\left(z\lambda/\pi W_o^2\right). \quad (4e)$$

N_{nm} normalizes the functions such that the power in a L-G beam mode is unity. That is,

$$1 = \int_0^{\infty}\int_0^{2\pi} r d\theta\, dr\, 2\Psi_{nm}\cdot\Psi_{nm}^{*}$$

which yields the recursive result $N_{nm}^2 = n!\sum_{q=0}^{m} N_{n-1\,q}^2$ with $N_{0m}^2 = 1/\pi W^2$.

The best fit L-G beam occurs when $R = L$, and choosing $W = 0.768a$ maximizes the power in the fundamental L-G mode [11]. This is a convenient choice because it means that fewer L-G modes are required to accurately describe the waveguide modes. The Bessel functions of the horn fields are now expressed as the summation of the L-G functions:

$$J_{n-1}\left(\gamma_{nm}\frac{r}{a}\right) e^{i(n-1)\theta + i\frac{kr^2}{2L}} = \sum_{p=0}^{\infty}\sum_{q=0}^{\infty} C_{pq}\Psi_{pq},$$

from which it follows that

$$C_{pq} = \frac{N_{pq}}{P_{nm}\pi a^2}\int_0^{\infty}\int_0^{2\pi} r\, d\theta\, dr \left(\frac{2r^2}{W^2}\right)^{n/2} L_{pq}\left(\frac{2r^2}{W^2}\right) J_{n-1}\left(\gamma_{nm}\frac{r}{a}\right)$$

$$\times \quad \exp\left(-\frac{r^2}{W^2} - i\frac{kr^2}{2R} + i\frac{kr^2}{2L} + i(n-1)\theta - ip\theta\right) \quad (5)$$

The phase slippage (Eq. 4e) is contained within the C_{pq}. Clearly, from Eq. 5 the

C_{pq} are trivial unless $p = n - 1$. Similarly, the coefficients of the $n + 1$ terms in the horn field (Eq. 2) are determined.

The present analysis considers a feed to be "slightly" overmoded if a few of the cylindrical waveguide modes propagate unattenuated through the waveguide. For example, the feeding waveguide has radius a_g, which, at a given frequency of radiation, supports the first three modes: The TE_{11}, the TM_{01}, and the TE_{21}. That is, the dimensionless frequency of radiation, $\gamma = a_g\omega/c$, is within the range $3.054 < \gamma < 3.832$ (at which point the TE_{02} and TM_{11} modes propagate. See Table 1).

Table 1: **Beam Mode Cut-off**

Mode	$\gamma_{\text{cut-off}}$
TE_{11}	1.84118
TM_{01}	2.40483
TE_{21}	3.05424
TE_{02}	3.831706
TM_{11}	3.83171

Table 2 lists the first 21 L-G coefficients ($C_{n-1\,m}$, $C_{n+1\,m}$) for each the TE_{11}, TM_{01}, and the TE_{21} waveguide modes. The total power in the first m modes up to 21 is also listed. Note that after 21 L-G modes 98.4% of the TE_{11} power is included; over 100 modes would have to be summed before 99.5% of the power would be included [11] (see Figure 2). The aperture and spillover efficiencies listed in Table 2 will be discussed in the next section.

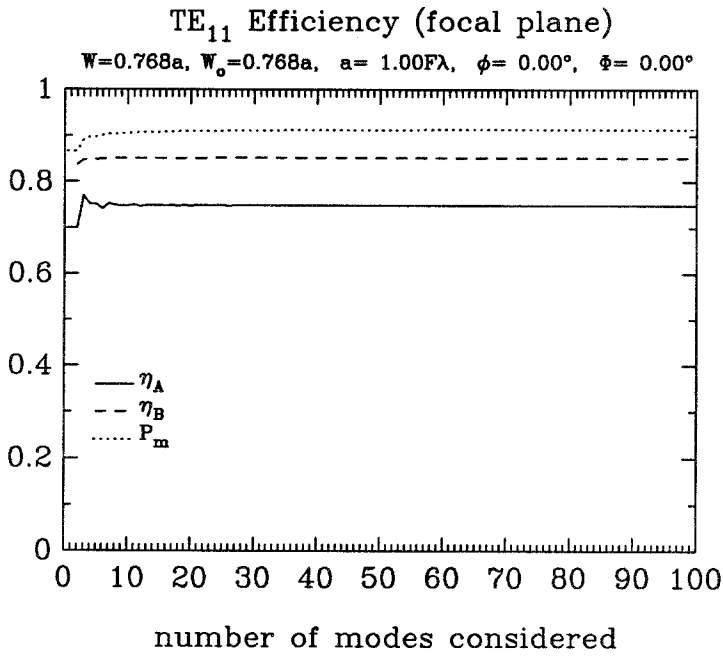

Figure 2: *The aperture and spillover efficiencies computed are plotted against the number of L-G modes included in the sum (Eq. 11 and Eq. 12). P_m is the amount of power included in the first m L-G modes. Twenty modes is enough to get a reasonable estimate of efficiency. This example is for the case of the infinite length horn ($\varphi = 0$) in the focal plane of the telescope.*

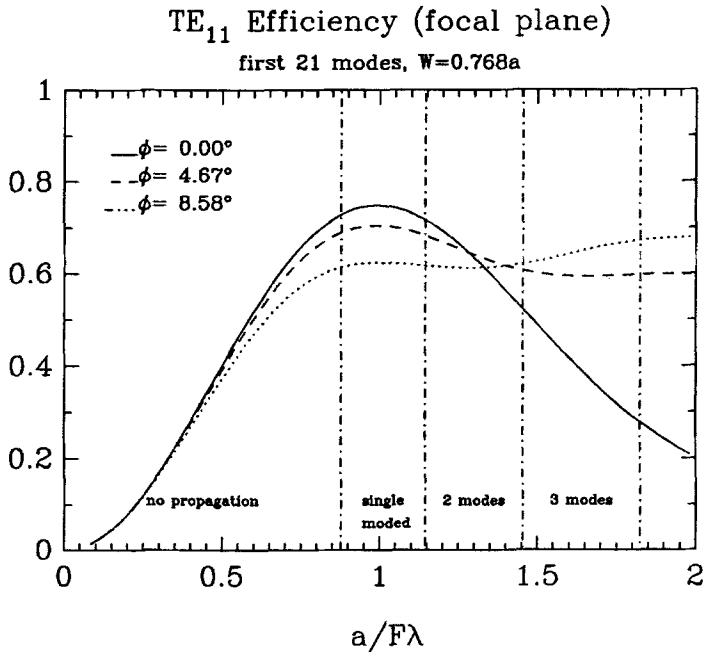

Figure 3: *The aperture efficiencies of three conical horns in the telescope focal plane are compared. Each is assumed to be fed by a single moded waveguide when the horn has maximum aperture efficiency ($a_m = F\lambda$ when $\gamma = a_g\omega/c = 2.1$ in all three cases). The three horns are the infinite horn ($\varphi = 0°$), the horn discussed in the text ($\varphi = 4.67°$), and an optimum horn [12] (horn of maximum gain for a given length; here, in comparison with the horn discussed in the text, the optimum horn of the same length would have flare angle $\varphi = 8.58°$).*

3 Efficiencies

3.1 Aperture Efficiency

The aperture efficiency is the ability of the antenna to couple to a point source on the sky. A point source at infinity produces a plane wave at the telescope aperture and its field profile therefore has no azimuthal (θ) dependence. Hence, only a feedhorn profile also having such a 'symmetric' profile can couple to the point source. Of the first three cylindrical wave modes (Table 1), only the TE_{11} can contribute to the aperture efficiency. The point source field is diffracted into the Airy pattern at the focal plane,

$$\vec{\mathrm{E}}_s = \frac{J_1(gr)}{gr}\hat{\boldsymbol{x}}\ , \tag{6}$$

where J_1 is the Bessel function of first order, $g = \pi/F\lambda$, and F is the f/D ratio of the telescope (here it is assumed to be a Gaussian Beam Telescope, wherein all lenses or mirrors are separated by the sum of their focal lengths[13,14]). An ideal aperture efficiency can be calculated by coupling the point source field directly to the horn field. This results in the maximum possible aperture efficiency which would be attained with perfect optics. The Fourier coefficients of Eq. 1 are then

$$A_{11} = \frac{1}{\pi a^2 P_{11}^{\mathrm{TE}}} \int_0^a \int_0^{2\pi} r d\theta dr\ \frac{J_1(gr)}{gr} J_0\left(1.841\frac{r}{a}\right) \tag{7}$$

The other coefficients of the first few waveguide modes are nought because only the TE_{1m} and TM_{1m} modes have a linearly polarized component to couple to the Airy profile, which is essentially a plane wave. For an infinitely long horn (*ie.* no phase correction at the horn mouth) Eq. 7 is maximized at $a = F\lambda$ for a coupling of $A_{11} = 0.865$ which gives the maximum possible aperture efficiency of $\eta_{\mathrm{Ap}} = 0.748$ when the horn is placed at the image of the focal plane (compare this to $\eta_{\mathrm{Ap}} = 0.837$ when the horn is in the aperture plane [11,12]).

For a practical horn, the focal plane does not occur at the horn mouth but at some distance within the horn, so Eq. 6 is first expressed as a sum of L-G beams at the waist ($z = 0$). The coefficients of the Airy profile in terms of the L-G beams can be calculated directly by taking the inner product of the Airy and L-G modes, but it is simpler to exploit the fact that L-G modes are unchanged by Fourier transformation except for a multiplicative term $(-1)^m$ [14] where m is the degree of the L-G mode, and note also that the beam waist radius at the aperture plane is related to that of the focal plane by

$$W_f = \lambda f/\pi W_{\mathrm{ap}}. \tag{8}$$

Table 2a: Laguerre-Gauss Coefficients and Efficiencies

TE_{11}

m	C_{0m}	P_{0m}	η_{Ap}	η_B	C_{2m}	P_{2m}	η_B
0	0.93092	0.86662	0.70004	0.83743	0.22095	0.048819	0.032147
1	-0.00016319	0.86662	0.70001	0.83743	0.095791	0.057995	0.035396
2	-0.15625	0.89104	0.76961	0.84700	-0.016674	0.058273	0.035482
3	-0.078191	0.89715	0.75091	0.84886	-0.065197	0.062524	0.036768
4	0.014460	0.89736	0.75120	0.84892	-0.060891	0.066232	0.037704
5	0.058322	0.90076	0.74124	0.84982	-0.030233	0.067146	0.037902
6	0.055583	0.90385	0.75233	0.85051	0.0039529	0.067161	0.037905
7	0.027983	0.90463	0.74827	0.85068	0.028146	0.067954	0.038072
8	-0.0037052	0.90465	0.74807	0.85068	0.037652	0.069371	0.038353
9	-0.026542	0.90535	0.74721	0.85082	0.033882	0.070519	0.038558
10	-0.035721	0.90663	0.75055	0.85106	0.021389	0.070977	0.038634
11	-0.032304	0.90767	0.74666	0.85123	0.0054864	0.071007	0.038639
12	-0.020475	0.90809	0.74902	0.85130	-0.0092722	0.071093	0.038653
13	-0.0052673	0.90812	0.74857	0.85131	-0.019839	0.071487	0.038716
14	0.0089384	0.90820	0.74817	0.85132	-0.024824	0.072103	0.038810
15	0.019169	0.90857	0.74815	0.85138	-0.024270	0.072692	0.038895
16	0.024037	0.90914	0.74912	0.85146	-0.019241	0.073062	0.038946
17	0.023545	0.90970	0.74752	0.85154	-0.011361	0.073191	0.038963
18	0.018698	0.91005	0.74905	0.85158	-0.0023972	0.073197	0.038963
19	0.011056	0.91017	0.74814	0.85160	0.0060517	0.073233	0.038968
20	0.0023343	0.91017	0.74831	0.85160	0.012764	0.073396	0.038989

The C_{nm} are the coefficients of the cylindrical beam modes to the Laguerre-Gauss beam modes Ψ_{nm}. P_{nm} is the total power in the first m Gaussian modes. η_{Ap} is the aperture efficiency when the first m Gaussian modes are considered; and η_B is the beam (or spillover) efficiency when the first m Gaussian modes are considered. The total spillover of the TE_{11} mode when looking at an extended thermal source is the sum of columns 5 and 8, $\eta_B = 0.891$. These efficiencies are for the case of an infinite length (flare angle of 0) horn: see also Figure 3.

Table 2b: Laguerre-Gauss Coefficients and Efficiencies

	TM_{01}			TE_{21}					
m	C_{1m}	P_{1m}	η_B	C_{1m}	P_{1m}	η_B	C_{3m}	P_{3m}	η_B
0	0.63775	0.40672	0.34657	0.86247	0.74385	0.63384	0.22916	0.52516	0.023088
1	0.12246	0.42172	0.35241	0.25556	0.80916	0.65926	0.17675	0.83756	0.034557
2	-0.11974	0.43605	0.35800	-0.073050	0.81449	0.66134	0.068877	0.88501	0.035785
3	-0.13845	0.45522	0.36371	-0.14359	0.83511	0.66748	-0.021223	0.88951	0.035898
4	-0.063283	0.45923	0.36471	-0.089137	0.84306	0.66948	-0.067628	0.93524	0.037047
5	0.017204	0.45952	0.36479	-0.0091024	0.84314	0.66950	-0.072405	0.98767	0.038223
6	0.063867	0.46360	0.36576	0.046965	0.84535	0.67002	-0.049955	0.10126	0.038708
7	0.071188	0.46867	0.36682	0.066016	0.84971	0.67093	-0.016718	0.10154	0.038760
8	0.050364	0.47121	0.36729	0.054843	0.85271	0.67150	0.014242	0.10174	0.038797
9	0.017211	0.47150	0.36735	0.027390	0.85346	0.67164	0.035146	0.10298	0.039022
10	-0.014682	0.47172	0.36739	-0.0028839	0.85347	0.67164	0.043279	0.10485	0.039346
11	-0.036741	0.47307	0.36763	-0.026549	0.85418	0.67176	0.039731	0.10643	0.039597
12	-0.045636	0.47515	0.36798	-0.039021	0.85570	0.67202	0.027843	0.10721	0.039713
13	-0.042167	0.47693	0.36825	-0.039846	0.85729	0.67226	0.011794	0.10735	0.039733
14	-0.029681	0.47781	0.36838	-0.031357	0.85827	0.67241	-0.0044648	0.10737	0.039736
15	-0.012565	0.47797	0.36840	-0.017265	0.85857	0.67245	-0.017868	0.10769	0.039782
16	0.0049342	0.47799	0.36841	-0.0014862	0.85857	0.67245	-0.026531	0.10839	0.039881
17	0.019464	0.47837	0.36846	0.012659	0.85873	0.67247	-0.029759	0.10927	0.040002
18	0.028922	0.47921	0.36858	0.022881	0.85925	0.67255	-0.027860	0.11005	0.040102
19	0.032490	0.48026	0.36872	0.028046	0.86004	0.67265	-0.021869	0.11053	0.040161
20	0.030457	0.48119	0.36883	0.028071	0.86083	0.67275	-0.013229	0.11070	0.040182

The C_{nm} are the coefficients of the cylindrical beam modes to the Laguerre-Gauss beam modes Ψ_{nm}. P_{nm} is the total power in the first m Gaussian modes. η_{Ap} is the aperture efficiency when the first m Gaussian modes are considered; and η_B is the beam (or spillover) efficiency when the first m Gaussian modes are considered. The spillover efficiency of the TM_{01} mode is $\eta_B = 0.738$, and for the TE_{21} mode it is the sum of columns 7 and 10, $\eta_B = 0.713$.

f is the focal length of the lens or mirror in the Gaussian Beam Telescope[14]. The integrals

$$\alpha_m = \frac{(-1)^m}{\pi(F\lambda/\pi)^2} \int_0^{2\pi} \int_0^{F\lambda/\pi} r d\theta dr \, \Psi_{0m} \tag{9}$$

with the substitution of Eq. 8 in Eq. 1 are more easily evaluated than the focal plane integrals which extend from 0 to infinity in r. Once the α_m have been determined, this L-G beam must be propagated up to the horn mouth which is simply done by modifiying the α_m by the phase slippage that occurs because the horn phase centre of radius occurs within the horn instead of at the horn mouth. Equations 1c and d can be inverted:

$$W_o = W\left[1 + \left(\pi W^2/\lambda L\right)\right]^{-\frac{1}{2}}, \tag{10a}$$

$$z = R\left[1 + \left(\lambda L/\pi W^2\right)\right]^2. \tag{10b}$$

Employing the orthogonality of the L-G beams, the coupling coefficients of Eq. 1 are then

$$A_{11} = \sum_{m=0}^{M} \alpha_m C_{0m}, \tag{11}$$

and the aperture efficiency is $\eta_A = A_{11}^2$. Table 2a lists the aperture efficiency for the case of the infinite length horn, and Column 2 of Table 3 lists the α_m. Enough L-G modes must be included in the sum (M in Eq. 11) to get an accurate calculation of the aperture efficiency. After about 20 modes the result changes only in the fourth decimal place (the value after 100 modes is $\eta_A = 0.7483$, see Figure 2.)

An example is given here which corresponds to the $855\mu m$ feedhorn of SCUBA which has a length of $40mm$. In this case the telescope beam is F4 (after reimaging the F12 beam of the JCMT). The horn mouth radius $a_m = 0.956F\lambda$ at $\lambda = 855\mu m$ is less than the optimum $a_m = F\lambda$ to allow for the horn wall thickness of $\sim 300\mu m$ and to ensure that the horn centres are $2F\lambda$ apart (the Nyquist sampling rate is $F\lambda/2$ so the horns are an integer number of "Nyquist" units apart). The feed is single moded at $855\mu m$ and has L-G beam width at the horn mouth of $W = 0.768a = 2.51mm$; the waist is $W_o = 0.665a = 2.17mm$ which occurs at $z = 3.07a = 10.0mm$ behind the horn mouth; the phase slippage is $\Phi = 0.525(2m + n) radians$. This gives an aperture efficiency of $\eta_A = 0.703$.

When the same feed is used at $\lambda = 700mm$ then the horn mouth radius is $a_m = 1.17F\lambda$; the beam width at the horn mouth is the same $W = 0.768a = 2.51mm$;

but the waist is now $W_o = 0.627a = 2.05mm$ at $z = 4.08a = 13.3mm$ behind the horn mouth, and the phase slippage is $\Phi = 0.615(2m + n)radians$. The aperture efficiency in this overmoded case is $\eta_A = 0.676$. There are two sources of loss in an overmoded system. The aperture efficiency is reduced because the horn mouth is too large, and the background loading is increased significantly which degrades the signal-to-noise of the device. This second effect is discussed in section 4.

3.2 Spillover

The beam efficiency in a Cassegrain telescope is defined as the fraction of power in the antenna beam which intercepts the image of an extended source through the telescope aperture. A source is considered to be extended if its angular extent exceeds the beam size of the telescope. The fraction of power which does not see the source on the sky "spills over" the telescope secondary mirror and looks at the entire sky surrounding the telescope beam. For this reason, the beam efficiency as defined here is often termed "spill over efficiency" in radio astronomy [15].

$$\eta_B = \sum_{m=0}^{M} \frac{C_{n-1m}^2}{\pi a^2} \int_0^a \int_0^{2\pi} r\, d\theta\, dr\, |\Psi_{n-1m}|^2 + \sum_{m=0}^{M} \frac{C_{n+1m}^2}{\pi a^2} \int_0^a \int_0^{2\pi} r\, d\theta\, dr\, |\Psi_{n+1m}|^2 . \tag{12}$$

The C_{nm} are the coefficients of the L-G functions, and M is the total number of L-G modes which are considered in the sum to approximate the field profile through the optical train, and n is the order of the cylindrical beam mode (Eqs. 1a and b) supported in the feed. The final four columns of Table 3 list the beam efficiencies associated with each L-G mode (*ie.* the integrals of Eq. 12) for the case of the infinite length horn. Finally, performing the summation of Eq. 12, the beam efficiency for each mode is calculated (see columns 5 and 8 of Table 2a, and columns 4, 7, and 10 of Table 2b). The overall spillover efficiency of the feedhorn depends on the number of waveguide modes propagating through the system, and on the nature of the signal to be measured (see next section). For the feedhorn system described in section 3.1 the spillover of the system when it is single moded ($\lambda = 855\mu m$) is $\eta_B = 0.902$. The spillover associated with each waveguide mode in the overmoded feed ($\lambda = 700\mu m$) is 0.811, 0.615, and 0.568 for the TE_{11}, TM_{01} and TE_{21} respectively.

Table 3: Laguerre-Gauss – Airy Coupling, and Beam Efficiencies

m	Ψ_{0m} – *Airy*	η_B			
	α_m	Ψ_{0m}	Ψ_{1m}	Ψ_{2m}	Ψ_{3m}
0	0.89877	0.96632	0.85212	0.65849	0.43964
1	0.10264	0.57907	0.38919	0.35410	0.36713
2	-0.25987	0.39179	0.39002	0.30666	0.25879
3	0.13714	0.30459	0.29772	0.30263	0.25049
4	0.011770	0.30402	0.25116	0.25245	0.25131
5	-0.098824	0.26439	0.25087	0.21651	0.22416
6	0.11543	0.22300	0.23780	0.21162	0.19471
7	-0.083778	0.21133	0.20904	0.21097	0.18323
8	0.031666	0.21124	0.18835	0.19796	0.18390
9	0.018706	0.20181	0.18319	0.17886	0.18231
10	-0.054093	0.18375	0.18323	0.16562	0.17267
11	0.069610	0.16851	0.17799	0.16169	0.15928
12	-0.066508	0.16219	0.16647	0.16194	0.14903
13	0.049638	0.16173	0.15438	0.15989	0.14487
14	-0.025242	0.16062	0.14690	0.15322	0.14476
15	-0.00065582	0.15523	0.14469	0.14410	0.14464
16	0.023238	0.14661	0.14472	0.13626	0.14171
17	-0.039341	0.13823	0.14341	0.13195	0.13585
18	0.047505	0.13289	0.13916	0.13087	0.12898
19	-0.047750	0.13100	0.13279	0.13097	0.12338
20	0.041211	0.13090	0.12643	0.13006	0.12030

The first 21 L-G coefficients of the Airy field pattern are listed for the case of the infinite length horn. (The waist,$W_o = 0.768a = 0.768F\lambda$, occurs at the horn mouth.) The spillover efficiencies in columns 3 to 6 are those associated with each L-G beam with $W = 0.768a$

4 Signal Measurement

In order to compute the signal coupled to the antenna by a particular source the spillover and the atmosphere transmission τ must be considered, as well as the aperture efficiency if it is a point source.

$$T_{\text{meas}} = \tau(\eta_B{}'\eta_{Ap}T_s' + \eta_B T_s) + (1-\tau)\eta_B T_{\text{atm}} + (1-\eta_B)T_{\text{atm}}$$

$$= \tau(\eta_B{}'\eta_{Ap}T_s' + \eta_B T_s) + (1-\tau\eta_B)T_{\text{atm}} \qquad (13)$$

where T_{meas} and T_{atm} are the equivalent Rayleigh-Jeans temperatures which is measured by the antenna, and emitted by the atmosphere respectively. T_s' and T_s are the temperatures emitted by the point source and an extended thermal source within the telescope beam. In the first term of Eq. 13 the spillover $\eta_B{}'$ is that associated with the part of the horn profile which couples to a point source (*eg.* column 6 of Table 2a for the infinite length horn).

An overmoded feed is most damaging to antenna efficiency because of increased background thermal loading. The Earth's atmosphere and any other black body or near black body source is an emission of random polarized radiation. Instantaneously, the antenna sees, on the average, radiation of any given polarization so each of the supported waveguide modes can couple to equal amounts of power. The spillover in this case is simply the average of those of the modes which propagate in the feed. For the feedhorn described in the last section $\eta_B = 0.902$, and when it supports the first two waveguide modes ($\lambda = 700\mu m$), $\eta_B = (0.811 + 0.615)/2 = 0.713$. The point source spillover is $\eta_B{}' = 0.860$ in the single moded case and $\eta_B{}' = 0.808$ in the overmoded case.

A typical calibrating source used from the JCMT might be Jupiter which emits as a point source black body of temperature ~150 K. The Earth's atmosphere is at ~275 K with transmission $\tau = \sim 0.70$ at $\lambda = 700\mu m$. The first term of Eq. 13 gives the source signal measured by the antenna: $0.70 \times 0.808 \times 0.676 \times 150\ K = \sim 55\ K$, and the rest gives the background loading: $(1 - 0.70 \times 0.713) \times 275\ K = \sim 140\ K$. So in a given time t, the detector measures ~195 K of which $\lesssim 25\%$ is signal from Jupiter, and $\gtrsim 75\%$ is background loading. When the same feed is used as a single moded device, then the source signal is now $0.70 \times 0.860 \times 0.703 \times 150\ K = \sim 65\ K$, and the background loading is $(1 - 0.70 \times 0.902) \times 275\ K = \sim 100\ K$. So in the single moded case, Jupiter accounts for ~40% of the flux entering the detector. Comparing the two cases, $(40\%/25\%)^2 = \sim 3$, implies that the integration time on the calibrating source Jupiter (the time required to obtain a given level of detection) is about 3 times longer if the feedhorn supports two waveguide modes.

5 Conclusions

A submillimetre feed was analyzed in order to estimate the aperture and beam efficiencies of a submillimetre astronomical receiver operating at non-optimum frequencies. The Submillimetre Common User Bolometer Array (SCUBA), to be installed on the James Clerk Maxwell Telescope, will measure flux from astronomical sources in four wavebands: $350\,GHz$ ($855\mu m$), $428\,GHz$ ($700\mu m$), $685\,GHz$ ($438\mu m$), and $857\,GHz$ ($350\mu m$). The two bolometer arrays mounted in the instrument are designed to operate with optimum efficiency at $438\mu m$ and $855\mu m$. At the shorter wavelengths the arrays consist of non-optimized feeds and one must consider the higher order beam modes which are then permitted to propagate in the system.

Efficiencies in the Cassegrain telescope were computed using Gaussian Beam Analysis after first determining the horn **E** field profile using the cylindrical waveguide modes as the "source" functions. The aperture efficiency (point source efficiency) and the beam efficiency (spillover efficiency) were both considered, and a particular case of the detection of Jupiter as a calibrating source was discussed.

The analysis shows that the $855\mu m$ array receiving $700\mu m$ radiation suffers a 2% reduction in aperture efficiency from 70% to 68%, and a 20% loss in beam efficiency from 90% to 71%. This last dominates the reduction in feedhorn performance since the background is normally brighter than the source, and a reduction in spillover efficiency implies increased background loading.

In terms of integration times for the example of Jupiter, this means that the telescope must look at a point source for roughly three times the duration when the receiver is overmoded at $700\mu m$ than it would if the antenna feed was optimized at that frequency. For source fluxes which are significantly smaller than that of Jupiter (as most interesting objects are), this difference between single and overmoded optics will become more severe as the background dominates more and more.

Overall, overmoded optics do reduce aperture efficiency as expected; nonetheless this may be an acceptable price to pay when a "quick & dirty" scheme for increasing the number of channels is desired on a receiver. In the case of the Submillimetre Common User Bolometer Array, this means the $700\mu m$ channel can be added to the instrument without manufacturing an array of bolometers dedicated to that frequency, and it will operate reasonably well.

Acknowledgements

The author is very grateful to Anthony Murphy for the many hours he spent answering questions, both in person and by electronic mail. Thanks are also due to the SCUBA project team at the Royal Observatory, Edinburgh, especially Walter Gear, Colin Cunningham, and Bill Duncan, and also the Department of Astronomy, Edinburgh.

References

1. Taub, J.J., Hindin, H.J., Hinckelmann, O.F., Wright, M.L., "Submillimeter Components Using Oversize Quasi-Optical Waveguide," *IEEE Trans. Microwave Theory & Techniques,* **vol. 11**, pp. 338-345, September 1963

2. Crenn, J.P., "Optical theory of Gaussian beam transmission through a hollow circular dielectric waveguide," *Appl. Opt.,* **vol. 21**, pp. 4533-41, December 1982

3. Belland, P., Crenn, J.P., "Matching of a Gaussian Beam into Hollow Oversized Circular Waveguides," *Int. J. IR & MM Waves,* **vol. 10**, pp. 1279-87, October 1989

4. Winston, R., "Light Collection within the Framework of Geometrical Optics," *J.Opt.Soc.Am.,* **vol. 60,** pp. 245-247, February 1970

5. Harper, D.A., Hildebrand, R.H., Stiening, R., Winston, R., "Heat Trap: An Optimized Far Infrared Field Optics System," *Applied Optics,* **vol. 15** pp. 53-60 January 1976

6. Clarricoats, P.J.B., Olver, A.D., *Corrugated Horns for Microwave Antennas,* Peter Peregrinus Ltd. on behalf of IEE, 1984

7. Olver, A.D., Jun Xiang, "Design of Profiled Corrugated Horns," *IEEE Trans. Antennas and Propagation,* **vol. 36,** pp. 936-940, July 1988

8. Cunningham, C.R., Gear, W.K., "The Submillimetre Common User Bolometer Array," *Proc. of SPIE Symp. Astronomical Telescopes & Instrumentation,* February 1990

9. Ludwig, A.C., "Radiation Pattern Synthesis for Circular Aperture Horn Antennas," *IEEE Trans. Antennas & Propagation,* **vol. 14**, pp. 434-40, July 1966

10. Kogelnik, H., Li, T., "Laser Beams and Resonators," *Proc. IEEE,* **vol. 54,** pp. 1312-29, October 1966

11. Murphy, J.A., "Aperture Efficiencies of Large Axisymmetric Reflector Antennas Fed by Conical Horns," *IEEE Trans. Antennas and Propagation,* **vol. 36** pp. 570-575, April 1988

12. King, A.P., "The Radiation Characteristics of Conical Horn Antennas," *Proc. IRE,* **vol. 38**, pp. 249-51, March 1950

13. Goldsmith, P.F., "Quasi-optical Techniques at Millimetre and Submillimetre Wavelengths," *Infrared and Millimetre Waves,* **vol. 6**, pp. 277-343, New York: Academic, 1982

14. Padman, R., Murphy, J.A., Hills, R.E., "Gaussian Mode Analysis of Cassegrain Antenna Efficiency," *IEEE Trans. Antennas & Propagation,* **vol. 35**, pp. 1093-1103, 1987

15. Christiansen, W.N., Högbom, J.A., *Radiotelescopes,* Cambridge University Press, 1985